Fast cortical microtubule array reorientation in *Arabidopsis* depends on KATANIN and is facilitated by SPIRAL3 and EB1.

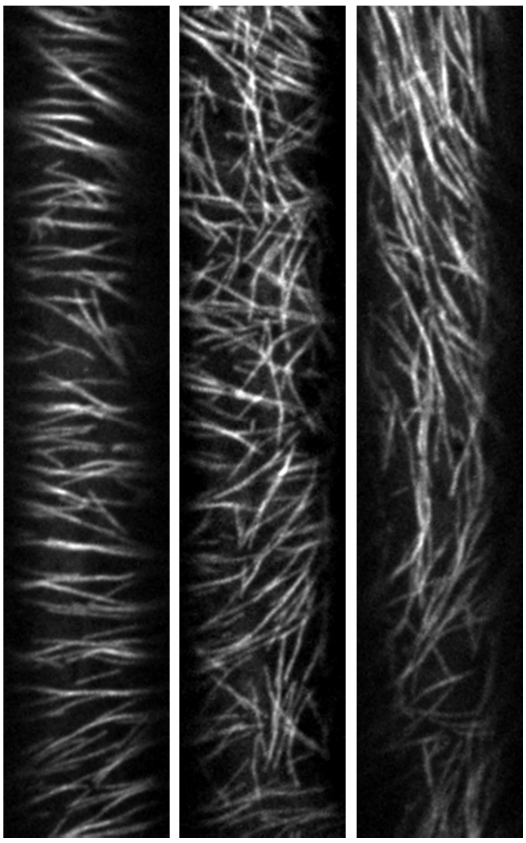

Msc thesis PCB-80439

Author: Anneke Hibbel

Date: 14-05-2011

Supervisors: Jelmer Lindeboom MSc & Dr. Tijs Ketelaar

Laboratory of Plant Cell Biology, Wageningen University

Fast cortical microtubule array reorientation in *Arabidopsis* depends on KATANIN and is facilitated by SPIRAL3 and EB1.

Anneke Hibbel

In elongating etiolated *Arabidopsis thaliana* hypocotyl epidermal cells, the cortical microtubule array is oriented transverse to the cell's elongation axis. In response to external stimuli such as wounding, ethylene and light, this transverse microtubule array progressively reorients to become longitudinal. The molecular mechanism behind array reorientation is unknown. Here, we set out to identify microtubule associated proteins (MAPs) whose microtubule modulating functions are involved in fast cortical microtubule array reorientation. We studied blue light-induced cortical microtubule array reorientation in etiolated hypocotyl epidermal cells of *A. thaliana* MAP mutants using live-cell imaging of fluorescently tagged microtubules. We show that the microtubule severing protein KATANIN is essential for fast cortical microtubule array reorientation. Without severing, the cortical microtubule array maintains its pre-existing transverse orientation. In absence of SPIRAL3, which mediates precise positioning of γ-tubulin complexes from which new microtubules are nucleated, cortical array reorientation proceeds at slower speed and shows altered angle distributions. Slower cortical array orientation is also observed in mutants of plus-end binding protein EB1. These results show that MAPs are essential for the process of fast cortical microtubule array orientation, which involves branched microtubule nucleation from pre-existing microtubules, severing of microtubules at sites of nucleation and crossover, and treadmilling.

INTRODUCTION

Plant cell growth results from cell wall expansion, which is driven by turgor pressure. This isotropic internal turgor pressure must be translated into an anisotropic growth pattern to create diverse plant cell types and shapes. In interphase cells, cortical microtubules are believed to guide cell morphogenesis by directing the deposition of cellulose microfibrils, thereby translating turgor pressure into controlled cell expansion (Green, 1962). Genetic and pharmacological approaches to disrupt microtubule organization have shown that cortical microtubule arrays are essential for the establishment of cell morphology (reviewed by Baskin, 2001). Microtubules are composed of α/β tubulin heterodimers, which are arranged in 13 linear proto-filaments that associate laterally into hollow cylinders with a diameter of 25 nm. Head-to-tail orientation of the α/β heterodimers results in microtubule polarity. B-tubulin is exposed at the faster growing plus-end, whereas α-tubulin is exposed at the minus-end of the

microtubules. The microtubule plus-ends stochastically alternate between prolonged periods of polymerisation (growth), depolymerisation (shrinkage) and pauses, a process termed dynamic instability (Desai & Mitchison, 1997). In plants, the microtubule minus-ends mainly alternate between pause and slow depolymerisation. The process of net gain at the plus end and net loss at the minus end was described as hybrid treadmilling (Shaw et al., 2003).

In animal and fungal cells, microtubule arrays are organized by microtubule organizing centres (MTOCs) such as centrosomes and spindle pole bodies. These MTOCs include γ-tubulin as part of a complex that spatially and temporally regulates the nucleation of microtubules (reviewed by Job et al. 2003). Higher plant cells, however, lack such MTOCs (reviewed by Bartolini & Gundersen, 2006). In interphase, microtubules are nucleated from multiple dispersed foci on the cortex and from existing microtubules (Wasteneys & Williamson, 1989; Shaw et al., 2003; Chan et al., 2003; Nakamura et al., 2010). Murata and colleagues (2005) proposed that γ-tubulin complexes shuttle between cytosol and cortical microtubule lattices, where they bind and nucleate new microtubules. These nascent microtubules either follow the axis of the pre-existing microtubule (Chan et al., 2009), or they branch off at an angle of 41.6 ± 8.2° with respect to the pre-existing microtubule (Murata, 2005) with a strong directional bias towards the plus-end of the pre-existing microtubule (Chan et al., 2009). Multiple microtubules can arise from the same microtubule associated nucleation site (Shaw et al., 2003). New microtubules can also arise at locations where two growing microtubules cross paths (Chan et al., 2009). Following nucleation, microtubules detach from the nucleation site and display unidirectional motility away from this site as a result of hybrid treadmilling rather than motor-driven microtubule translocation (Shaw et al., 2003). The detachment from the nucleation site is caused by the severing action of the microtubule associated protein (MAP) KATANIN (Nakamura & Hashimoto, 2009). Through plus-end polymerisation and hybrid treadmilling, microtubules can encounter each other. Depending on the level of lateral cortical attachment, individual microtubules can change direction of growth (Sainsbury et al., 2008). The level of cortex attachment also influences the range of encounter angles and the frequency of interactions between microtubules. Depending on the angle of this encounter and the level of cortex attachment, microtubule-microtubule interactions result in crossing-over with or without microtubule reorientation, induced catastrophe, severing or bundling (Wasteneys & Ambrose, 2009). When the angle of encounter is <40º, the incoming microtubule is likely to redirect its trajectory and to bundle by lateral association with the pre-existing microtubule (zippering) (Dixit & Cyr, 2004). Bundles of microtubules tend to be more stable than individual microtubules, indicating that bundles function as positional and orientational traps (Dixit & Cyr, 2004; Paradez et al., 2006; Ehrhardt & Shaw, 2006;

Shaw et al., 2003). At steeper angles than 40º, most microtubules experience crossing-over or catastrophe (catastrophic collisions) (Dixit & Cyr, 2004; Wightman & Turner, 2007). Modelling of microtubule dynamics showed that catastrophic collisions are sufficient to facilitate formation of aligned cortical microtubule arrays (Tindemans et al., 2010). The cortical microtubule array in elongating cells such as etiolated hypocotyl epidermis cells is oriented transversely to the elongation axis. New microtubules are not readily nucleated in the preferred transverse orientation of the cortical microtubule array. Rather, they polymerise preferentially diagonal with respect to the elongation axis of the cell (J. Lindeboom, personal communication) and are progressively aligned parallel to each other into a transverse array configuration (Wasteneys & Ambrose, 2009). This transverse cortical microtubule array can be reoriented by 90º to become aligned parallel to the elongation axis of the cell as a response to developmental cues and environmental stimuli (Baskin, 2001; Granger & Cyr, 2001). In elongating tissues, the transition from transverse to a longitudinal orientation is usually slow and related to termination of cell growth (Baskin, 2001). However, complete cortical microtubule array reorientations from transverse to longitudinal plane have been observed in as little as ten minutes in response to external cues (Paradez et al., 2006). This array reorientation is not established by depolymerisation of microtubules in the original orientation followed by polymerisation of microtubules in the new orientation. Instead, microtubules progressively move into the new global configuration in a continuous process during which different alignments coexist (Yuan et al., 1994; Granger & Cyr, 2001). The molecular mechanism behind this cortical microtubule array reorientation is not yet known. Shaw and colleagues (2003) reported that translocation, the lateral and axial sliding of microtubules into new positions, does not occur in *Arabidopsis* cortical microtubule arrays. Thus, kinesin motor proteins are not expected to play an important role in cortical microtubule array reorientation. Interactions between MAPs and microtubules, however, potentially do govern cortical microtubule array organisation through their effect on microtubule dynamics (Dixit & Cyr, 2004; Paradez et al., 2006; Lindeboom et al., 2008). Here, we set out to identify microtubule associated proteins (MAPs) whose microtubule modulating functions are involved in fast cortical microtubule array reorientation. We analysed blue light-induced cortical microtubule array reorientation in etiolated hypocotyl epidermal cells of *A. thaliana* MAP mutants using live-cell imaging of fluorescent protein-labelled microtubules. We studied SPIRAL3 mutants, in which microtubule nucleating angles are wider and more divergently distributed (Nakamura & Hashimoto, 2009), to determine the role of precise positioning of γ-tubulin nucleation complexes in cortical microtubule array reorientation. In addition, we investigated the microtubule severing protein KATANIN (Burk et al., 2001) to identify the importance of severing during cortical microtubule array reorientation. Finally, we

studied plus-end binding MAPs EB1 (Chan et al., 2003) and SPIRAL1 (Nakajima et al., 2004) which are believed to influence microtubule dynamic instability (Busch & Brunner, 2004; Sedbrook, 2004; Katsuki et al., 2009), to assess the effect of microtubule stability on cortical microtubule array reorientation. We show that high intensity blue light induces fast phototrophin mediated cortical microtubule array reorientation. In absence of KATANIN, the cortical microtubule array maintains its pre-existing transverse orientation. SPIRAL3 influences microtubule angle distributions during cortical microtubule array reorientation, as well as the speed of this array reorientation. Slower cortical array orientation is also observed in plus-end binding protein EB1 mutants. Our results provide evidence that fast cortical microtubule array reorientation depends on the precise positioning of γ-tubulin complexes on pre-existing microtubules by SPIRAL3 and microtubule severing by KATANIN.

METHODS

Transgenic lines.

All plants used in this study were *A. thaliana* ecotype Columbia (Col-0), except for *spiral3 and katanin* mutants, which were ecotype Wassilewskija (Ws). Two constructs were used for imaging of cortical microtubules: 35S::YFP:TUA5 (Shaw et al., 2003*)* and 35S::GFP:TUB6 (Nakamura et al., 2004). Mutant line seeds of YFP::TUA5 *cry1 cry2,* YPF::TUA5 *phot1 phot2,* YFP:TUA5 *eb1b,* YFP:TUA5 *eb1a eb1b eb1c*, YFP-TUA5 *spiral1* and YFP:TUA5 *eb1b spiral1* were provided by Viktor Kirik (Illinois State University, USA). Mutant lines YFP:TUA5 *eb1a eb1b eb1c spiral1,* GFP:TUB6 *spiral3*, and GFP:TUB6 *katanin* were provided by Ryan Guiterrez (Carnegie Institution for Science, Stanford, USA).

Growth.

A. thaliana seeds were surface sterilized, stratified for 4 days at 4 °C, and sown in Petri dishes on 1.0% agar-solidified half strength Murashige and Skoog (MS) salts medium (Sigma-Aldrich) at pH=5.7. After 1 hour of light exposure, seedlings were grown in darkness for 64–72 hours at 25 °C.

Specimen mounting.

Seedlings were mounted under safelight conditions in sterile water between a 24 ×50 mm cover glass and a 1-mm thick 1.0% agarose pad affixed to a 24 ×24 mm cover glass, which stabilized the sample and prevented mechanical damage.

Confocal microscopy.

Imaging of plants expressing 35S::YFP:TUA5 and 35S::GFP:TUB6 was performed on a system featuring a CSU-X1 spinning disk head (Yokogawa), Eclipse Ti inverted microscope (Nikon), 100x/1.4 NA oil immersion objective, Evolve 512 EMCCD camera (Photometrics) and 1.2x lens between the spinning disk unit and camera. Excitation switching and shuttering was performed by a multi-channel AOTF device (AA Opto-Electronic Company). YFP and GFP were excited at 491 nm. Emission filtering was accomplished with band pass filters (530/50 nm for both GFP and YFP; Chroma Technology). For all imaging experiments, focal shift was corrected automatically by the Perfect Focus System (Nikon).

Imaging of cortical microtubule array reorientation in *A. thaliana* hypocotyl epidermis cells.

Epidermal hypocotyl cells of etiolated *A. thaliana* seedlings were selected based on location with respect to the apical hook. We imaged cells in which the orientation of the cortical microtubule array was transverse, located in the two elongating cell files directly underneath the division zone of the apical meristem. Time-lapse imaging of 35S::YFP:TUA5 or 35S::GFP:TUB6 labelled cells was performed in the optical plane of the cell cortex adjacent to the outer tangential wall. Acquisitions were performed with 400-ms exposures and 8.2 mW optical fibre output. Time series were obtained over 60 minutes at 10-s intervals.

General image processing.

All image processing was performed using ImageJ software (Rasband, W. S, US National Institutes of Health, Bethesda, MD, USA). Angle values were measured per pixel and assigned to 9º bins using the rotating filter plug-in (J. Lindeboom, R. Gutierrez, K. Shundyak & D. Ehrhardt).

Analysis of cortical microtubule nematic order and angle distributions.

For each time-series, the fraction of pixels per bin was calculated per frame and plotted as contour plot of angle fractions over time. Nematic order (S) values per frame were calculated using formula (1) and plotted per time-series as graph of nematic order over time.

$$S(frame) = \sqrt{\langle sin2\alpha \rangle^2 + \langle cos2\,\alpha \rangle^2} \qquad (1)$$

Where $\langle sin2\alpha \rangle = \frac{\sum length_i sin\alpha_i}{\sum_j length_j}$

The angle of preferred orientation θ per frame was calculated using formula (2), and plotted per time-series as graph of preferred angle over time.

$$preferential\ angle\ \theta(frame) = arccos\left(\frac{S+\langle cos2\alpha \rangle}{\sqrt{2S^2+2\langle cos2\alpha \rangle S}}\right). \qquad (2)$$

RESULTS

Blue light induces fast cortical microtubule array reorientation in etiolated *A. thaliana* Col-0 hypocotyl epidermis cells.

Epidermis cells in the upper hypocotyl of *A. thaliana* Col-0 seedlings, expressing 35S::YFP:TUA5 to label microtubules, were excited at 491 nm by spinning disk confocal microscopy for one hour at 10-s interval. Within this hour, 15 out of 18 cells completed cortical microtubule array reorientation from the pre-existing transverse orientation to a new configuration with longitudinal orientation. On average, cortical microtubule arrays reoriented over a 75° angle (figure 1).

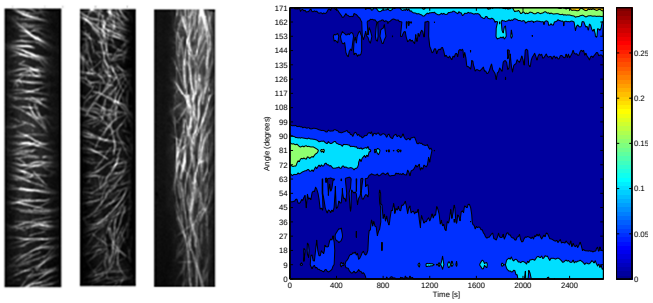

Figure 1. Blue light-induced cortical microtubule array reorientation in Col-0 seedlings expressing 35S::YFP:TUA5. A). Panels show the cortical microtubule array of a Col-0 etiolated hypocotyl epidermis cell at t=0 (left panel), t=30 minutes (centre), and t=60 minutes (right panel) after onset of 491 nm blue light exposure. B). Contour plot of cortical microtubule angle distributions during Col-0 cortical microtubule array reorientation. Graph shows single cell data.

We measured angle distributions of cortical microtubules over time and found that cortical microtubule array reorientation typically follows a pattern consisting of three phases: 1) decreasing nematic order, 2) increasing nematic order 3) constant nematic order (figure 2). We calculated average speed of array reorientation from onset of light-induction (t=0) until the end of reorientation (figure 3, indicated as reorientation phase). Corresponding to the array reorientation, the angle of preferred orientation of the cortical array as a whole changed over time at a mean speed of 3.8 ± 2.6 degrees/minute (table 2).

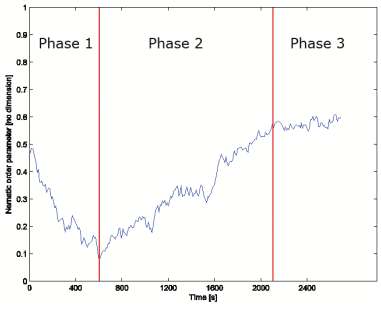

Figure 2.

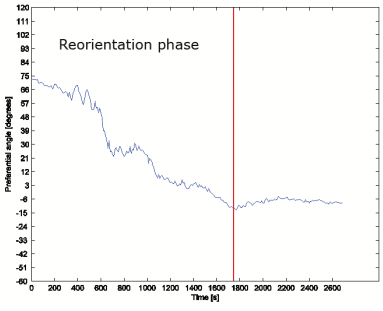

Figure 3.

Figure 2. Nematic order during Col-0 cortical microtubule array reorientation. (value between 0 and 1; 0 represents complete disorder and 1 represents complete order). Graph shows single cell data.

Figure 3. Preferential angle during array reorientation. Graph shows single cell data.

Phototrophin is involved in fast cortical microtubule array reorientation.

Next, we assessed blue light-induced cortical microtubule array reorientation in cryptochrome and phototrophin photoreceptor mutants, to investigate whether cortical array reorientation is dependent on blue-light photoreceptors. At onset of light exposure, the cortical array of Col-0, *cry1 cry2* and *phot1 phot2* were equally ordered (table 1). During cortical array reorientation, *cry1 cry2* seedlings did not differ from Col-0 with respect to angle distributions and speed of array reorientation. In *phot1 phot2*, the average speed of cortical array reorientation was significantly reduced compared to Col-0 (table 2). Reduced array reorientation speed in *phot1 phot2* mutants was also reflected by lower nematic order at t=40 minutes after onset of light induction (n=9, Mann-Whitney U Test, $p<0.05$), at which time Col-0 on average reached constant nematic order. In summary, phototrophin is involved in fast blue light-induced reorientation of the cortical microtubule array from a transverse to a longitudinal orientation with respect to the elongation axis of the cell.

Table 1. Cortical microtubule array nematic order at onset of light-induction in Col-0 and mutants.

Plant line		Nematic order at t=0	Independent Samples Mann-Whitney U Test
Col-0	(n=18)	0.38 ± 0.15	
cry1 cry2	(n=13)	0.37 ± 0.15	p=0.890
phot1 phot2	(n=10)	0.43 ± 0.11	p=0.308
eb1b	(n=11)	0.50 ± 0.15	p=0.147
eb1a eb1b eb1c	(n=11)	0.34 ± 0.18	p=0.707
spr1	(n=19)	0.41 ± 0.16	p=0.753
eb1b spr1	(n=8)	0.36 ± 0.07	p=1.000
eb1a eb1b eb1c spr1	(n=13)	0.56 ± 0.12	p=0.002 *
spr3	(n=11)	0.35 ± 0.12	p=0.492
katanin	(n=14)	0.38 ± 0.09	p=0.985

Plus-end MAPs influence the speed of cortical microtubule array reorientation.

To gain insight in MAP executed microtubule modulating functions important for cortical microtubule array reorientation, we studied MAP mutants during blue light exposure. At onset of light exposure, nematic order within the cortical array of plus-end MAP mutants *eb1b*, *eb1a eb1b eb1c, spiral1* and *eb1b spiral1* was equal to Col-0. *eb1a eb1b eb1c spiral 1* showed a significantly higher ordering than Col-0 at onset of light-exposure (table 1).

For each mutant, we calculated average speed of array reorientation (table 2). We found that *spiral1* reorients at the same speed as Col-0. Mean cortical array reorientation was slower than Col-0 in the plus-end MAP mutants *eb1b*, *eb1a eb1b eb1c*, *eb1b spiral1* and *eb1a eb1b eb1c spiral1*.

Table 2. Average speed of cortical microtubule array reorientation in Col-0 and mutants.

Plant line		Average speed degrees/minute	Independent Samples Mann-Whitney U Test
Col-0	(n=18)	3.80 ± 2.60	
cry1 cry2	(n=15)	3.76 ± 3.46	p=0.735
phot1 phot2	(n=10)	1.07 ± 0.63	p=0.000 *
eb1b	(n=11)	1.61 ± 1.37	p=0.004 *
eb1a eb1b eb1c	(n=11)	1.76 ± 0.95	p=0.004 *
spr1	(n=14)	2.78 ± 2.31	p=0.107
eb1b spr1	(n=8)	1.95 ± 0.43	p=0.006 *
eb1a eb1b eb1c spr1	(n=13)	1.10 ± 1.08	p=0.000 *
spr3	(n=11)	0.90 ± 1.00	p=0.000 *
katanin	(n=14)	0.35 ± 0.47	p=0.000 *

Pairwise comparisons revealed that *eb1b* did not differ significantly from *eb1a eb1b eb1c* and *eb1b spiral1*. *eb1b spiral1* reoriented faster than *eb1a eb1b eb1c spiral1*, whereas *eb1a eb1b eb1c* did not significantly differ from *eb1a eb1b eb1c spiral1* (table 3). These results suggest that plus-end MAP EB1 is involved in fast cortical microtubule array reorientation, whereas SPIRAL1 alone does not influence the speed of array reorientation.

Table 3. Pairwise comparisons of average speed of cortical microtubule array reorientation in plus-end MAP mutants.

Plant lines	Independent Samples Mann-Whitney U Test
eb1b <> eb1b spr1	p=0.051
eb1b <> eb1a eb1b eb1c	p=0.456
eb1b spr1 <> eb1a eb1b eb1c spr1	p=0.020 *
eb1a eb1b eb1c <> eb1a eb1b eb1c spr1	p=0.110

Dispersed nucleation angles in MAP mutant *spiral3* cause altered angle distributions and decreased speed of array reorientation.

We investigated the role of branched nucleation on cortical microtubule array reorientation. SPIRAL3 plays a role in the precise positioning of γ-tubulin containing foci from which new microtubules nucleate on pre-existing microtubules. In the *spiral3* mutant, nucleating angles are wider and more divergently distributed (Nakamura & Hashimoto, 2009). This mutant shows helical cortical microtubule arrays and severe helical growth (Nakamura & Hashimoto, 2009). We found that at onset of light-induction, nematic order within the cortical microtubule array of *spiral3* seedlings expressing 35S::GFP:TUB6 was equal to Col-0 (table 1). The typical initial decrease in nematic order during array reorientation as seen in Col-0 is absent in *spiral3* seedlings. Instead, nematic order slightly increases during array reorientation. The cortical array appears to reorient starting from the transverse alignment via an oblique orientation towards a longitudinal orientation with respect to the long axis of the cell (figure 5). On average, s*piral3* reoriented significantly slower than Col-0 (table 2). These results show that cortical microtubule array reorientation still occurs when nucleating angles are wider and more divergently distributed. However, the reorientation process proceeds with altered angle distributions and at reduced speed, suggesting that precise positioning of γ-tubulin nucleation complexes by *spiral3* is important for fast cortical microtubule array reorientation.

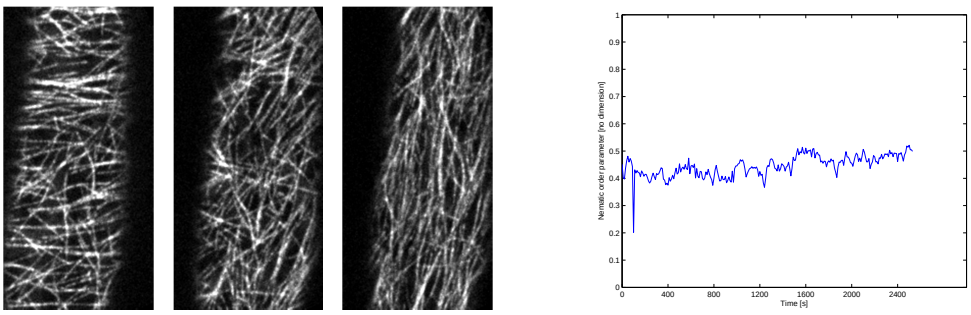

A. B.

Figure 5. Altered angle distribution during cortical microtubule array reorientation in *spiral3* seedlings expressing 35S::GFP:TUB6. A). Panels show the cortical microtubule array of a *spiral3* etiolated epidermal hypocotyl cell at t=0 (left panel), t=32 minutes (centre), and t=60 minutes (right panel) after onset of 491 nm blue light exposure. B). Nematic order during *spiral3* cortical microtubule array reorientation. Graph shows single cell data.

Severing activity of KATANIN is essential for cortical microtubule array reorientation.

After nucleation, microtubules are released from the γ-tubulin nucleation complex by the severing action of KATANIN. To investigate the role of severing in cortical microtubule array reorientation, we studied *katanin* mutants expressing 35S::GFP:TUB6. In *katanin* plants cell expansion is disrupted, leading to reduced plant cell and organ length (Burk et al., 2001). At onset of light-induction, nematic order in *katanin* did not differ significantly from Col-0 (table 1). Upon blue light-induction, *katanin* mutants fail to undergo cortical microtubule array reorientation (figure 6 & 7).

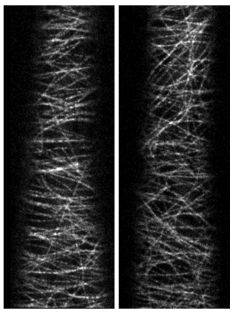

Figure 6. The pre-existing cortical microtubule array is maintained in *katanin* seedlings expressing 35S::GFP:TUB6. Panels show the cortical microtubule array of *katanin* etiolated epidermal hypocotyl cell at t=0 (left panel) and t=60 minutes (right panel) after onset of 491 nm blue light exposure.

Over the course of the experiment, nematic order steadily decreases in this mutant as a result of branched nucleations. However, the preferential angle of orientation remains fixed around 90° with respect to the elongation axis of the cell, indicating that the pre-existing transverse array is maintained (figure 7). *katanin* has an 11x lower average speed of blue light induced cortical microtubule array reorientation, which is significantly slower than Col-0 (table 2). These results show that the severing function of KATANIN is essential for the breakdown of the pre-existing transverse cortical array and for establishing a new array order during fast cortical microtubule array reorientation.

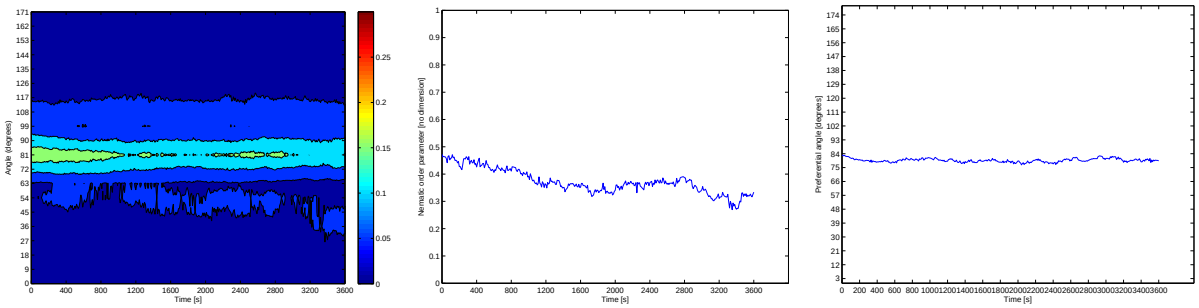

Figure 7. Cortical microtubule array reorientation is hampered in *katanin* mutants. A). Contour plot of cortical microtubule angle distributions during cortical microtubule array reorientation in *katanin*. B). Nematic order during array reorientation. C). Preferential angle during array reorientation. Graphs show single cell data.

DISCUSSION

A number of studies have reported cortical microtubule array reorientation as a response to developmental cues and environmental stimuli (Baskin, 2001; Granger & Cyr, 2001). However, the mechanism behind this array reorientation has remained unknown. Here we show that the photoreceptor phototrophin is involved in high intensity blue light-induced fast cortical microtubule array reorientation in etiolated *A. thaliana* hypocotyl epidermis cells. This reorientation process is dependent on the microtubule severing MAP KATANIN and facilitated by SPIRAL3 and EB1.

KATANIN severs nascent microtubules at their microtubule-bound nucleation sites (Nakamura & Hashimoto, 2009), as well as at locations of crossing over, followed by shrinkage of the new lagging end. This provides a mechanism for the removal of unaligned microtubules (Wightman and Turner, 2007) and enables new microtubule orientations. In *katanin* mutants we did observe branched nucleation of new microtubules from pre-existing transverse microtubules following the onset of light-induction. Without the severing function of KATANIN, however, newly nucleated microtubules cannot be released from the nucleation complex, nor undergo treadmilling. Therefore, the primary transverse array order does brake down in *katanin*. Subsequently, this mutant fails to establish a new orientation of aligned microtubules.

In addition to microtubule severing, we show that the precise positioning of the γ-tubulin containing complex on pre-existing microtubules by SPIRAL3 is pivotal for the progression of cortical array reorientation. Murata and colleagues (2005) suggested that during cortical reorientation, new microtubules are nucleated on pre-existing microtubules as branches through controlled positioning of the γ-tubulin complexes. Our data suggest that wider and more divergently distributed nucleation angles due to incorrectly placed γ-tubulin complexes in *spiral3* (Nakamura & Hashimoto, 2009) alter and slow down the process of array reorientation. Branched nucleation at wider angles from transverse mother microtubules may lead to an increased probability of steep-angle encounters between newly nucleated microtubules and obstructing transverse microtubules. Steep-angle encounters increase the probability of induced catastrophes (Dixit & Cyr, 2004; O. Zaitseva, personal communication) and thus may slow down the progress of induced cortical microtubule array reorientation.

We also found reduced speed of cortical array reorientation in EB1 mutants. Mal3, the EB1 orthologue in *Schizosaccharomyces pombe*, stabilizes microtubules by suppressing catastrophe through inhibition of lattice depolymerisation and by enhancing rescue (Busch & Brunner, 2004; Katsuki et al., 2009). We observed increased cytoplasmic background fluorescence in EB1 mutants after onset of array reorientation, which could

indicate higher levels of cytoplasmic YFP:TUA5 as a result of reduced microtubule stability in the absence of EB1. The analysis of microtubule stability in EB1 mutants is beyond the scope of this study. Nevertheless, slower cortical microtubule array reorientation in EB1 mutants putatively results from reduced microtubule stability, which may increase the probability of induced catastrophe upon microtubule-microtubule interactions. Starting from a transverse array orientation, a higher number of branched microtubules is then required in order to obtain and maintain enough microtubules in the new angle of preferred orientation. Thus, the observed reduced reorientation speed in SPIRAL3 and EB1 mutants may result from altered outcomes of angle-dependent microtubule-microtubule interactions in these mutants. Moreover, absence of EB1 might reduce growth speed of microtubules. In yeast, binding of Mal3 to microtubule plus-ends increases microtubule growth speed in a dose dependent manner and reduces the lifetime of the conformational state of tubulin from the recognized state at growing ends to the state tubulin adopts in the lattice (Maurer et al., 2011). EB1 might facilitate microtubule growth in a similar way. The reduced reorientation speed of the cortical microtubule array in EB1 mutants could thus be a result of altered microtubule growth dynamics. Furthermore, EB1 is thought to recruit additional MAPs to the microtubule plus-end (Sedbrook, 2004). Pairwise comparisons of EB1 mutants in combination with *spiral1* suggest that the proteins EB1a and/or EB1c may interact with SPIRAL1 during cortical microtubule array reorientation. Alternatively, functional redundancy could exist between SPIRAL1 and EB1a and/or EB1c, explaining the aggravated phenotype of the quadruple mutant *eb1a eb1b eb1c spiral1* during cortical array reorientation. *spiral1* undergoes cortical microtubule array reorientation at the same speed as Col-0, suggesting that SPIRAL1 alone does not play a role in the reorientation process. Alternatively, possible functional redundancy within the SPIRAL1 multi-gene family (Sedbrook et al., 2004) could mask the influence of SPIRAL1 in cortical array reorientation.

The cortical microtubule array reorients from a transverse to a longitudinal orientation in response to different environmental stimuli (Baskin, 2001; Granger & Cyr, 2001). Soga and colleagues (2010) reported that ACC, the immediate precursor of ethylene, induces reorientation of cortical microtubules from transverse to longitudinal directions within 2 hours after start of treatment, preceding changes in growth anisotropy. Transcript levels of γ-tubulin complex and KATANIN were increased transiently within 0.5 h after the start of ACC treatment and returned to control level 2 hours after the start of treatment. These findings suggest that the number of the branched microtubules may be increased through up-regulation of γ-tubulin complex genes, which together with the observed

increase in KATANIN expression could facilitate reorientation of the cortical microtubule array (Soga et al., 2010). Here, we report that high intensity blue light induces SPIRAL3 and KATANIN dependent cortical microtubule array reorientation in epidermis cells in the upper elongation zone of the *A. thaliana* hypocotyl. However, the time span between photoreceptor activation and onset of microtubule reorientation is in the range of minutes. Therefore, it is unlikely that altered transcription levels account for this fast cortical array reorientation. Rather, posttranslational modifications may convey signal transduction from phototrophin to the cytoskeleton. PHOT1 and PHOT2 have intrinsic protein kinase activity (reviewed by Briggs & Christie, 2002). Hence, phosphorylation of target proteins such as potentially SPIRAL3 may trigger altered microtubule dynamics leading to array reorientation. Future actinomycin D and cycloheximide pharmacological experiments could be used to rule out the role of respectively transcription and translation in blue light-induced fast cortical microtubule array reorientation.

The mechanistic insights obtained from our analysis of cortical microtubule array reorientation in MAP mutants may aid the interpretation of the cortical microtubule array reorientation process in Col-0. Altered angle distributions in *spiral3* seedlings during light-induced cortical microtubule array reorientation suggest that initiation of cortical microtubule array reorientation in Col-0 is induced by altered microtubule nucleation angles upon light-induction. A small number of microtubules deviate from the dominant transverse orientation in the cortical microtubule array at onset of light-induction, suggesting that most microtubule nucleations are along existing microtubules. An induced switch to branched nucleation from transverse mother microtubules would lead to decreasing array order, as is observed in the first phase of Col-0 array reorientation. Following microtubule plus-end polymerisation, these newly nucleated microtubules will encounter and interact in an angle-dependent manner with other microtubules, which are predominantly in the transverse orientation. Upon microtubule-microtubule encounters, severing of either the incoming microtubule (Wightman and Turner, 2007), or the obstructing microtubule may occur following crossover (Chan 2009). If oblique microtubules, potentially resulting from branched nucleations, start to outnumber transverse microtubules, angle-dependent microtubule-microtubule interactions between transverse and oblique microtubules would eventually yield an array in which the preferred angle of orientation is no longer transverse but oblique. Since we have no indication that the transverse array is polarized with microtubules plus-ends pointing in the same direction, local oblique arrays are expected, which lead to low order of the cortical array. From microtubules in the now dominant oblique orientations, on-going branched nucleations could finally lead to an increasingly longitudinal orientation of the

array, a phase characterized by increasing order. Finally, microtubules in the now dominant longitudinal orientation encounter each other at shallow angles, forming parallel and antiparallel bundles that stabilize the new cortical array orientation, which is reflected in constant order within the Col-0 cortical microtubule array. In summary, our results suggest that the mechanism underlying fast cortical microtubule array reorientation involves branched microtubule nucleations on pre-existing microtubules, subsequent severing of microtubules at sites of nucleation and crossing over, and microtubule treadmilling. Detailed analysis of the number of branched nucleations and severing events per μm microtubule per time unit should reveal whether blue light-induction of cortical microtubule array reorientation indeed leads to higher numbers of these events.

Here we present evidence that fast cortical microtubule array reorientation depends on the precise positioning of γ-tubulin complexes on pre-existing microtubules by SPIRAL3 and microtubule severing by KATANIN. Since the KATANIN and SPIRAL3 plant lines used in this study were ecotype Ws, whereas all other plant lines were ecotype Col-0, cortical microtubule array reorientation should additionally be studied in Ws wild type plants to rule out any confounding ecotype effects. Furthermore, the overview of MAPS involved in cortical microtubule array reorientation presented in this study is incomplete. Future studies should focus on the contribution of MAPS such as CLASP-1 to reveal the role of microtubule attachment to the plasma membrane in cortical microtubule array reorientation. Finally, investigation of the role of fast cortical microtubule reorientation in plant cell growth and morphogenesis may provide new insights in the biological function of this process.

Acknowledgements

I am grateful to Jelmer Lindeboom MSc and Dr. Tijs Ketelaar for their supervision during my time as master-thesis student at the Laboratory of Plant Cell Biology, WUR, from September 2010 until May 2011. Thanks to Dr. David Ehrhardt for our discussion on my results. Thanks to Dr. Viktor Kirik and Ryan Guiterrez MSc for providing transgenic seeds. Thanks to the Plant Cell Biology group members for their inspiring input. Last but not least, thanks to Henk and Siglinde Hibbel for funding my education over the last 25 years.

References

Bartolini, F. & Gundersen, G.G (2006).Generation of noncentrosomal microtubule arrays. J Cell Sci. 119: 4155-63.

Baskin, T.I. (2001). On the alignment of cellulose microfibrils by cortical microtubules: a review and a model. Protoplasma 215, 150-171.

Briggs, W.R. & Christie, J.M. (2002). Phototropins 1 and 2: versatile plant blue-light receptors. Trends in Plant Science 7: 204-210.

Burk, D.H., Liu, B., Zhong, R.Q., Morrison, W.H., and Ye, Z.H. (2001). A katanin-like protein regulates normal cell wall biosynthesis and cell elongation. Plant Cell 13, 807-827.

Busch, K.E. & Brunner, D. (2004). The microtubule plus end-tracking proteins mal3p and tip1p cooperate for cell-end targeting of interphase microtubules. Curr Biol. 14(7): 548-59.

Chan, J., Calder, G.M., Doonan, J.H., and Lloyd, C.W. (2003). EB1 reveals mobile microtubule nucleation sites in *Arabidopsis*. Nature Cell Biology 5, 967-971.

Chan, J., Sambade, A., Calder, G., and Lloyd, C. (2009). *Arabidopsis* Cortical Microtubules Are Initiated along, as Well as Branching from, Existing Microtubules. Plant Cell 21, 2298-2306.

Desai, A., and Mitchison, T.J. (1997). Microtubule polymerization dynamics. Annual Review of Cell and Developmental Biology 13, 83-117.

Dimitrov, A., Quesnoit, M., Moutel, S., Cantaloube, I., Pous, C., and Perez, F. (2008). Detection of GTP-Tubulin Conformation in Vivo Reveals a Role for GTP Remnants in Microtubule Rescues. Science 322, 1353-1356.

Dixit, R., and Cyr, R. (2004). Encounters between dynamic cortical microtubules promote ordering of the cortical array through angle-dependent modifications of microtubule behavior. Plant Cell 16, 3274-3284.

Dixit, R., and Cyr, R. (2004). The cortical microtubule array: From dynamics to organization. Plant Cell 16, 2546-2552.

Ehrhardt, D.W., and Shaw, S.L. (2006). Microtubule dynamics and organization in the plant cortical array. Annual Review of Plant Biology 57, 859-875.

Granger, C.L., and Cyr, R.J. (2001). Spatiotemporal relationships between growth and microtubule orientation as revealed in living root cells of *Arabidopsis thaliana* transformed with green-fluorescent-protein gene construct GFP-MBD. Protoplasma 216, 201-214.

Green, P.B. (1962). Mechanism for Plant Cellular Morphogenesis. Science 28; 1404-5.

Job, D., Valiron, O., and Oakley, B. (2003). Microtubule nucleation. Current Opinion in Cell Biology 15, 111-117.

Katsuki M., Drummond, D.R., Osei, M. & Cross, R.A. (2009). Mal3 masks catastrophe events in Schizosaccharomyces pombe microtubules by inhibiting shrinkage and promoting rescue. J Biol Chem. 284(43):29246-50.

Lindeboom, J., Mulder, B.M., Vos, J.W., Ketelaar, T., and Emons, A.M.C. (2008). Cellulose microfibril deposition: coordinated activity at the plant plasma membrane. Journal of Microscopy-Oxford 231, 192-200.

Maurer, S.P., Bieling, P., Cope, J., Hoenger, A. & Surrey, T. (2011). GTPgammaS microtubules mimic the growing microtubule end structure recognized by end-binding proteins (EBs). Proc Natl Acad Sci 108(10):3988-93.

Murata, T., Sonobe, S., Baskin, T.I., Hyodo, S., Hasezawa, S., Nagata, T., Horio, T., and Hasebe, M. (2005). Microtubule-dependent microtubule nucleation based on recruitment of gamma-tubulin in higher plants. Nature Cell Biology 7, 961-U952.

Nakajima, K., Furutani, I., Tachimoto, H., Matsubara, H., and Hashimoto, T. (2004). SPIRAL1 encodes a plant-specific microtubule-localized protein required for directional control of rapidly expanding *Arabidopsis* cells. Plant Cell 16, 1178-1190.

Nakamura M., Naoi K., Shoji T., Hashimoto T. (2004). Low concentrations of propyzamide and oryzalin alter MT dynamics in *Arabidopsis* epidermal cells. Plant Cell Physiol. 45: 1330–1334.

Nakamura, M., Ehrhardt, D.W., and Hashimoto, T. (2010). Microtubule and katanin dependent dynamics of microtubule nucleation complexes in the acentrosomal *Arabidopsis* cortical array. Nature Cell Biology. Advance online publication.

Nakamura, M., and Hashimoto, T. (2009). A mutation in the *Arabidopsis* gamma-tubulin containing complex causes helical growth and abnormal microtubule branching. J. Cell Sci. 122, 2208-2217.

Paradez, A., Wright, A. &Ehrhardt, D.W. (2006). Microtubule cortical array organization and plant cell Morphogenesis. Current Opinion in Plant Biology 2006, 9:571–578.

Sainsbury, F., Collings, D.A., Mackun, K., Gardiner, J., Harper, J.D.I., and Marc, J. (2008). Developmental reorientation of transverse cortical microtubules to longitudinal directions: a role for actomyosin-based streaming and partial microtubule-membrane detachment. Plant J. 56, 116-131.

Sedbrook, J.C. (2004). MAPs in plant cells: delineating microtubule growth dynamics and organization. Curr Opin Plant Biol. 7(6):632-40.

Sedbrook, J.C., Ehrhardt, D.W., Fisher, S.E., Scheible, W.R., and Somerville, C.R. (2004). The *Arabidopsis* SKU6/SPIRAL1 gene encodes a plus end-localized microtubule interacting protein involved in directional cell expansion. Plant Cell 16, 1506-1520.

Shaw, S.L., Kamyar, R., and Ehrhardt, D.W. (2003). Sustained microtubule treadmilling in *Arabidopsis* cortical arrays. Science 300, 1715-1718.

Soga, K., Yamaguchi, A., Kotake, T., Wakabayashi, K. & Hoson, T. (2010). Transient increase in the levels of γ-tubulin complex and katanin are responsible for reorientation by ethylene and hypergravity of cortical microtubules.Plant Signal Behav. [Epub ahead of print]

Tindemans, S.H., Hawkins, R.J., and Mulder, B.M. (2010). Survival of the Aligned: Ordering of the Plant Cortical Microtubule Array. Physical Review Letters 104.

Wasteneys, G.O. (2002). Microtubule organization in the green kingdom: chaos or selforder? Journal of Cell Science 115, 1345-1354.

Wasteneys, G.O., and Ambrose, J.C. (2009). Spatial organization of plant cortical microtubules: close encounters of the 2D kind. Trends in Cell Biology 19, 62-71.

Wasteneys, G.O. & Williamson, R.E. (1989). Reassembly of microtubules in *Nitella tasmanica*: quantitative analysis of assembly and orientation. European Journal of Cell Biology 50, 76-83.

Wasteneys, G.O. & Williamson, R.E. (1989). Reassembly of microtubules in *Nitella tasmanica*: assembly of cortical microtubules in branching clusters and its relevance to steady-state microtubule assembly. Journal of Cell Science 93; 705-714.

Wightman, R., and Turner, S.R. (2007). Severing at sites of microtubule crossover contributes to microtubule alignment in cortical arrays. Plant J. 52, 742-751.

Yuan, M., Shaw, P.J., Warn, R.M., and Lloyd, C.W. (1994). Dynamic Reorientation of Cortical Microtubules, from Transverse to Longitudinal, in Living Plant-Cells. Proceedings of the National Academy of Sciences of the United States of America 91, 6050-6053.

APPENDIX A.

Details on the experiments described below are recorded in the lab journal of Anneke Hibbel, September 2010 - April 2011.

Transformation of 35::GCP2:3xGFP into *A. thaliana* Col-0 plants expressing 35S::mCherry:TUA5

Binary plasmid 35S::GCP2:3xGFP was provided by R. Gutierrez (Carnegie Institution Department of Plant Biology, Stanford). The binary plasmid was introduced into *A. thaliana* Col-0 plants expressing 35S::mCherry:TUA5 by *Agrobacterium* mediated transformation to generate double-labelled lines. Seeds were harvested and grown in Petri dishes on 0.7% agar-solidified half-strength Murashige and Skoog (MS) salts medium (Sigma-Aldrich) at pH=5.7 supplemented with kanamycin and 0.5 hygromycin antibiotics to select for positive transformants. Seedlings were grown on soil in a climate chamber for further processing by Jelmer Lindeboom.

Genotyping of c*lasp-1* single mutants.

Previously, Jelmer Lindeboom crossed *clasp-1* with *A. thaliana* Col-O plants expressing 35S::YFP:TUA5. DNA was extracted from rosette leaf material using the Edwards prep DNA extraction protocol. Mutant lines were identified by PCR. No *clasp-1* homozygous mutants were obtained from these crosses, therefore heterozygous *clasp1* seeds were re-sown on soil for further processing by Jelmer Lindeboom.

Genotyping of c*lasp-1 eb1b* and *spiral1 clasp-1* double mutants.

Seeds of *clasp-1 eb1b* expressing 35S::YFP:TUA5 and *spiral1 clasp1* expressing 35S::YFP:TUA5 lines were provided by V. Kirik (Carnegie Institution Department of Plant Biology, Stanford). Seeds were grown in Petri dishes on 0.7% agar-solidified half-strength Murashige and Skoog (MS) salts medium (Sigma-Aldrich) at pH=5.7 supplemented with Basta antibiotics to select for YFP expression. Subsequently, seedlings were grown on soil in a climate chamber. DNA was extracted from rosette leaf material using the Edwards prep DNA extraction protocol. Mutant lines were identified by PCR, yielding positive identification of *spiral1 clasp1* homozygous double mutants and c*lasp-1 eb1b* homozygous double mutants.